"ART" IN X-RAY TOMOGRAPHY: IMAGE NOISE REDUCTION

Marina Chukalina
Institute of Microelectronics Technology RAS
142432 Chernogolovka
Moscow District, Russia
marina@ipmt-hpm.ac.ru

Dmitry P. Nikolaev
Institute for Information Transmission Problems RAS
Bol'shoj Karetnyj lane, 19
101447, Moscow, Russia
dimonstr@iitp.ru

Alexandre Simionovici
Lab. Geophysique Interne & Tectonophysique
UMR5559, Maison des Geosciences, BP 53
38041 Grenoble Cedex 9, France
Alexandre.Simionovici@ujf-grenoble.fr

KEYWORDS
X-ray tomography, algebraic reconstruction technique, solution polygon, image domain, image noise reduction.

ABSTRACT

Reduction of the object dose by reducing X-ray exposure has the inevitable consequence of increasing statistical noise in the projections. A set of projections with a 10% noise, collected during the test experiment at the Institute of Crystallography RAS, were used to reconstruct a water phantom. Two different reconstruction approaches (Algebraic Reconstruction Technique (ART) and Filtered Back Projections (FBP)) were implemented. The reconstructed images also had about 10 % noise in both cases. Median filtering within each ART iterative step and averaging over images, updated and preserved during the final iteration made it possible to lower the image noise to 3%. For ART calculations, the RegART software package developed by the authors was used.

INTRODUCTION

CT is used in medicine as a diagnostic tool and as a guide for interventional procedures. X-ray slice data is generated using an X-ray source that rotates around the object; X-ray sensors are positioned on the opposite side of the circle from the X-ray source. The data stream representing the varying radiographic intensity transmitted to the detectors on the opposite side of the circle during each sweep is then computer processed to calculate cross-sectional estimates of the radiographic density. Sweeps cover 360 or just over 180 degrees in conventional machines (wikipedia).

Mathematically, there are two major classes of tomographic reconstruction techniques (Naterrer 1981, Kak and Slaney 1988). One class, the transform based methods, uses the Fourier-slice theorem. The other type of methods employs iterative procedures to reconstruct an image. The most widely used of them is the algebraic reconstruction technique (Gordon 1974). This technique is less efficient than the transform based methods but they have several advantages. They can be used with irregular sampling geometries, incomplete noisy data sets and may incorporate curved ray paths (Wan et al.2003, Schubert 2004).

When measured projections have a low signal/noise ratio, a high quality of the reconstructed images is very difficult to obtain. Using additional sub-iteration of filtering in the ART and averaging over images, updated and preserved during the final iteration, we improved image quality.

In the next section, the experimental setup and projections acquisition are described. The algebraic reconstruction technique details follow them. Our RegART software description and comparison of the images reconstructed with the RegART and with the filtered back-projection technique completes this paper.

EXPERIMENTAL SETUP

The scheme of the experiment carried out at the Institute of Crystallography RAS is typical. The x-ray beam generated by the laboratory source passed through the Si 220 monochromator (to cut the 0.7A line), and the beam collimator. At a distance of 1 m from the 1 mm-wide and 1 mm-high laboratory source, a sample was mounted on a tomography stage with the horizontal rotation axis (Asadchkov 2005). The sample was a 10.5 mm polypropylene capillary of 1.6 mm wall thickness, filled with water. The object-to detector distance was 0.1m. The image was detected with a linear (1024 pixel with 14 bits dynamic range) system. The effective pixel size was 0.1 mm. After flat field normalization of the projections, the tomograms were reconstructed. 84 projections were collected in the parallel mode (Fig.1).

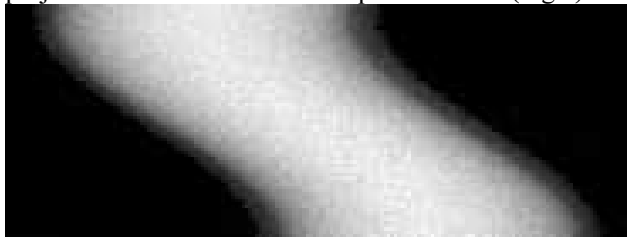

Fig.1. A set of collected tomography projections.

Proceedings 21st European Conference on Modelling and Simulation
Ivan Zelinka, Zuzana Oplatková, Alessandra Orsoni ©ECMS 2007
ISBN 978-0-9553018-2-7 / ISBN 978-0-9553018-3-4 (CD)

ALGEBRAIC RECONSTRUCTION TECHNIQUE

Mathematical description of the projection formation

We use the Cartesian coordinate system to describe the projection formation. The equation for the line *AB* in Fig.2 is

$$x\cos\varphi + y\sin\varphi = \xi \quad (1)$$

Let $f(x,y)$ describe the linear attenuation coefficient. Then the transmission function of the pencil beam *AB* is

$$I(\varphi,\xi) = I_0(\varphi,\xi)\cdot \cdot \exp(-\iint dxdyf(x,y)\delta(x\cos\varphi + y\sin\varphi - \xi)), \quad (2)$$

where I_0 is the intensity of the initial pencil beam and δ is the Dirac delta-function. Now let introduce a new function $p(\varphi,\xi) = \ln\left(\frac{I_0(\varphi,\xi)}{I(\varphi,\xi)}\right)$ and rewrite the expression (2):

$$p(\varphi,\xi) = \iint dxdyf(x,y)\delta(x\cos\varphi + y\sin\varphi - \xi) \quad (3).$$

The function $p(\varphi,\xi)$ is known as the Radon transform of the function $f(x,y)$. When combined a set of integrals forms a projection. We used a parallel scheme. The parallel projection is a collection of pencil beam integrals (3) for a constant φ.

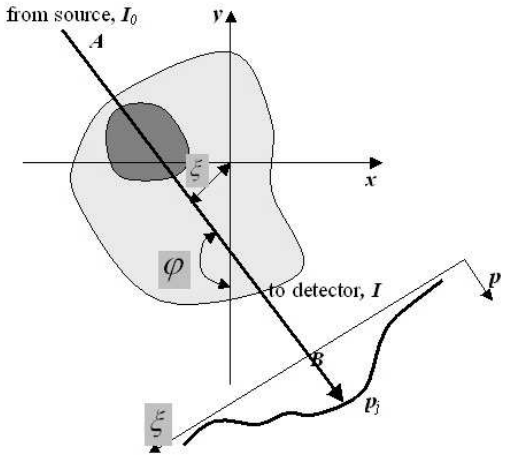

Fig.2. Parallel tomography scheme.

The aim of the next section is to introduce the algebraic approach for image reconstruction.

Image and projections representation.

In Fig.3 we have imposed a square grid on the image $f(x,y)$. Let assume that in each pixel the function $f(x,y)$ is constant. Consequently, we will search the solution in the space of the piecewise constant functions. Let f_i denote a constant value in the *i*th pixel and *N* be the total number of pixels. For the algebraic reconstruction technique the X-ray is a bar running through the image plane. In our case the ray width is approximately equal to the pixel size (Fig.3).

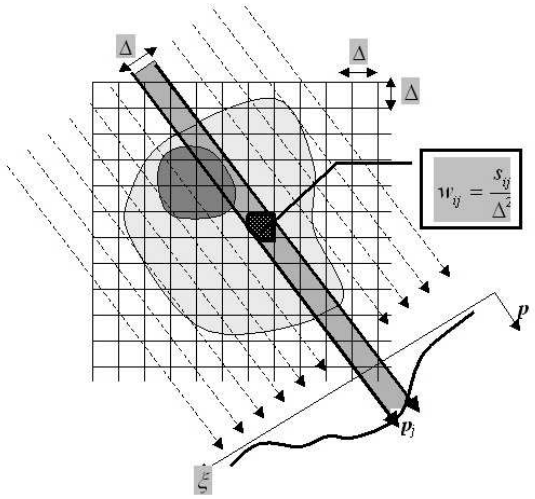

Fig.3. Parallel tomography scheme. Discreet representation.

The intensity p_j will now be called a ray sum. The relation between p_j and $\vec{f}$ may be expressed as

$$p_j = \sum_{i=1}^{N} f_i w_{ij},\ j = 1,...M \quad (4)$$

where *M* is the total number of rays (in all projections) and w_{ij} is the weighting factor that represents the contribution of the *i*th pixel to the *j*th ray sum.

Iteration scheme

For large *N* and *M* there exist iterative methods to solve the system (4). They are based on the "method of projections" first proposed by Kaczmarz (Kaczmarz 1937). An image, presented by $\vec{f}$, may be considered to be a single point in an *N*-dimensional space. Each of the above linear equations (1) defines a hyperplane. The unique solution to these equations is the intersection of all hyperplanes.

Let $\vec{f}^k$ be the estimated solution at the *k*-th iteration. The iteration scheme is

$$\vec{f}^{k+1} = \vec{f}^k + \gamma\frac{p_j - \left(\vec{f}^k, \vec{w}_j\right)}{\left(\vec{w}_j, \vec{w}_j\right)}\vec{w}_j. \quad (5)$$

Here γ is the so-called relaxation parameter (Ros et al. 1996). It shows (Censor et al. 1983) that the limits of cyclic subsequences generated by the method approach a weighted least squares solution of the system when the relaxation parameter goes to zero. This point minimizes the sum of squares of Euclidean distances to the hyperplanes of the system.

RegART algorithm description

Weight matrix

For computer implementation of the algorithm we first calculate a set of weight sparse matrices $w_j, j = 1,...M$ for all rotation angles φ (Fig. 3). In many ART implementations the weights are simply replaced by 1's and 0's depending upon whether the center of pixel is within the fine ray. This makes the

implementation easier. This approximation although easy to implement often leads to artifacts in the reconstructed images (Chukalina et al 2005). The value of the weight depends on the point-spread function (PSF) which describes the response of an imaging system to the point object. In our package, there are three regimes of calculations: '0-1' regime; regime illustrated in Fig.3 (s_{ij} is the square of the *i*-th pixel part covered by the *j*-th fine beam); regime with the 2D Gaussian PSF).

Initial guess

The initial guess denoted by $\vec{f}^0$ is assigned a value of zero. It was shown (Ming and Ge 2003) that from any initial guess the sequence generated by the ART converges to a weighted least square solution. This initial guess is projected on the hyperplane represented by the first equation in (5) to yield $\vec{f}_1^0$. The subscript indicates how many hyperplanes are included in the $\vec{f}^0$ correction process. After each projection to a hyperplane, the estimated image $\vec{f}^0$ is updated. The first sub-iteration is finished if the correction over all hyperplanes is finished.

Projection access scheme

A lot of projection access schemes are discussed in the literature (Guan and Gordon 1996). To minimize the influence of two neighbor hyperplanes on each other we used the following scheme:

$$p(\varphi_1,\xi_1), p\left(\varphi_1+\frac{\pi}{2},\xi_1\right), p(\varphi_1,\xi_2), p\left(\varphi_1+\frac{\pi}{2},\xi_2\right),\ldots$$

$$p\left(\varphi_1,\xi_{N/2}\right), p\left(\varphi_1+\frac{\pi}{2},\xi_{N/2}\right),\ldots p\left(\varphi_M+\frac{\pi}{2},\xi_{N/2}\right).$$

Two sub-iterations

Because the projections are noisy, the intersection of the hyperplanes is not a point in the *N*-dimensional space but a polygon. Each iteration projects the estimated solution to a polygon wall area. On the other hand, the solution sought for belongs to the image class sub-space. The size, shape and position of the sub-space depend on the accuracy of the image description (accuracy of the image model). The image sub-space and the polygon can intersect or be close to each other. The regularization operator brings the estimated solution from the polygon wall area to the image sub-space (Cheremuhin and Chulichkov 2005). The space of the piecewise constant functions is well suited for the description of the tomography images. However, it is very difficult to construct the projector which brings an estimated solution to this image sub-space. We have taken the space of piecewise smooth functions as the image space, i.e. if the function belongs to this space it will belong to the same space after the median operator was implemented. Then the median filtering operator can be used as the projector from the polygon wall area to the image sub-space. Following Davidson (Davidson et al. 2006), we have implemented the median filtering as the second sub-iteration. It is known that the median filtering reduces speckle noise and salt and pepper noise. Its edge-preserving nature makes it useful in the cases where edge blurring is undesirable. It should be mentioned that the type of projector depends on the chosen image sub-space and in the general case it could be of any kind.

Nonnegativity constraint

The nonnegativity constraint is reinforced, when instead of $f<0$ we set $f=0$.

One iteration is completed after the full set of measurements has been processed.

In the next iteration, $\vec{f}^k$ is projected onto the hyperplane represented by the first equation in (5), and successively onto the rest of the hyperplanes in (5), then the filtering is implemented and so on until the last iteration.

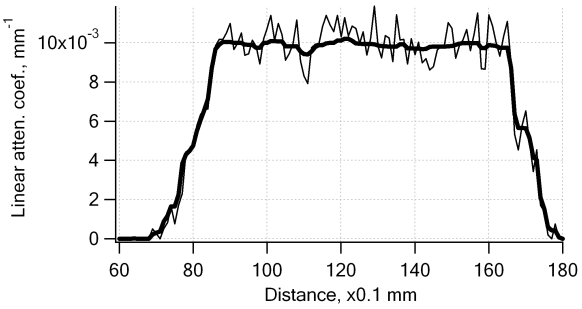

Fig.4. Two crossections of the reconstructed water phantom. The black line is the reconstruction with median filtering; the gray line is the reconstruction without filtering.

Final step

In the last iteration, all images $\vec{f}_1^{last},\ldots\vec{f}_{N*M}^{last}$ are saved. The final step of the algorithm is the averaging over these images to exclude the specific influence of the last hyperlane projection. The result of the reconstruction with the RegART algorithm is presented in Fig.5.

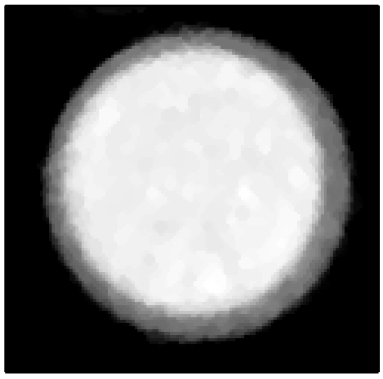

Fig.5. Water phantom reconstructed with the RegART.

The average value of the water coefficient is 0.098 ± 0.003 mm^{-1}, reference value is 0.099 mm^{-1} (Henke et al. 1993). In Fig 6, the results of the filtered back-projection algorithm implementation (Buzmakov 2005) is shown. With noisy data and few projection

angles, the RegART algorithm shows better reconstruction results as compared with FBP.

SUMMARY AND OUTLOOK

We proposed to include new additional steps in the classical algebraic reconstruction algorithm They yield an estimated image by means of the median filtering. The final step of the algorithm is the averaging over these images to exclude the specific influence of the last hyperlane projection.

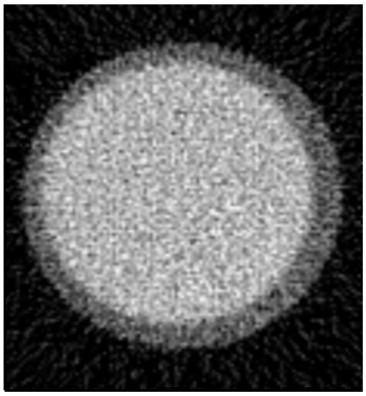

Fig.6. Water phantom reconstructed with FBP.

We plan to optimize the speed of this procedure by including the algorithm developed for the Haugh transform fast calculations (Karpenko et al. 2005)

This work is supported by the RFBR 06-01-22001, 06-02-16117, PICS 3470. M. Chukalina thanks the Institute of Crystallography RAS for additional support.

REFERENCES

Asadchikov V., V. Babak, A. Buzmakov et al. 2005. "X-ray difractometer with a source-detector moving system." *Engineering and experimental devices* 3, 1-9 (in Russian).

Buzmakov A. 2005. *Microtomography of the biological samples with sub-millimeter resolution on 0.7-2.2A.* Moscow State University diploma. Supervisors: A. Andreev, V. Asadchikov.

Censor Y., P.B. P. Eggermont, D. Gordon. 1983. "Strong underrelaxation in Kaczmarz's method for inconsistent systems." *Numerische Mathematik* 41, no. 1, 83-92.

Cheremuhin E., A.I. Chulichkov. 2005. "Usage of the measurement computer systems in tomography." *Issue of Calc. Math. and Math. Phys*. 45, no.4, 741-752.

Chukalina M., A. Buzmakov, R. Senin, V. Asadchikov. 2005. "X-ray tomography: artifacts reasons." *Proc. of the Nanophysics and Nanoelectronics Symposium*, 294-295 (in Russian).

Davidsov J.L., Ch. A. Garcia-Stewart, K.B. Ozanyan, P. Wright, S. Pegrum, H. McCann. "Image reconstruction for chemical species tomography with inregular and sparse beam array." *Photon 06. Book of Proceedings*. 4-7 September, University of Manchester. http://www.photon06.org/OPD%20P2.9.doc

Gordon. R. 1974. "A tutorial on art (algebraic reconstruction technique)." *IEEE Trans. Nucl. Sci*. 21,78-93.

Guan H., R. Gordon. 1996. "Computed tomography using algebraic reconstruction techniques (ARTs) with different projection access schemes: a comparison study under practical situations." *Phys. Med. Biol.* 41**,** 1727-1743.

Henke B.L., E.M. Gullikson, and J.C. Davis. 1993. *X-ray interactions: photoabsorption, scattering, transmission, and reflection at E=50-30000 eV, Z=1-92*. Atomic Data and Nuclear Data Tables Vol. **54,** no.2.

Kak A.C., M. Slaney. 1988. *Principles of Computerized Tomographic imaging.* IEEE Press, NY.

Ming J., W. Ge. 2004. "Convergence of the simultaneous algebraic reconstruction technique (SART)." *IEEE trans. image proc.* 12, no.8, 957-961.

Karpenko S.M., Nikolaev D.P., Nikolayev P.P., Postnikov V.V. 2005. "General method for fast Hough transforms construction." *Proc. of IEEE AIS'05 and CAD-2005*, Moscow. V. 2, 313-318.

Natterer F. 1981. *Mathematical aspects of computerized Tomography*. Springer.

Ros D., C. Falcon, I. Juvells, J. Pavia. 1996. "The influence of a relaxation parameter on SPECT iterative reconstruction algorithms." *Phys. Med. Biol*. 41, No.5, 925-937.

Schubert F. 2004. http:// www.ndt.net / article / ewgae2004 / html / htmltxt / l58schubert.htm .

Wan X., Y.Gao, Q. Wang, S. Le, S. Yu. 2003. "Limited-angle optical computed tomography algorithms." *Optical engin*. 42, no.9, 2659-2669.

AUTHOR BIOGRAPHIES

MARINA V. CHUKALINA received her PhD in physics at the Institute of Microelectronics Technology RAS where she has been working since 1988. Her interests include the development of signal and image processing tools for X-ray Microscopy and Tomography. Her Web-page can be found at http://www.ipmt-hpm.ac.ru/english/labs/lcd/.

DMITRY P. NIKOLAEV received his PhD degree at Moscow State University in 2004 in physics. He has been a research scientist at the Institute for Information Transmission Problems RAS since 2000. His research activities are in the areas of computer vision with primary application to colour image understanding.

ALEXANDRE S. SIMIONOVICI received his PhD in Atomic Physics in 1988 at the Univ. of Paris - Orsay. He is a professor of geochemistry at the Univ. of Grenoble. His research interests include: Earth and Planetary Sciences, Environmental Sciences, Microanalysis, Coupled X-ray techniques: spectroscopy, tomography, diffraction, Novel data analysis and treatment methods.